Extremize Optical Chiralities through Polarization Singularities

Weijin Chen,[1,*] Qingdong Yang,[1,*] Yuntian Chen,[1,2,†] and Wei Liu[3,‡]
[1]School of Optical and Electronic Information, Huazhong University of Science and Technology, Wuhan, Hubei 430074, People's Republic of China
[2]Wuhan National Laboratory for Optoelectronics, Huazhong University of Science and Technology, Wuhan, Hubei 430074, People's Republic of China
[3]College for Advanced Interdisciplinary Studies, National University of Defense Technology, Changsha, Hunan 410073, People's Republic of China

(Received 13 January 2021; accepted 27 May 2021; published 24 June 2021)

Chiral optical effects are generally quantified along some specific incident directions of exciting waves (especially for extrinsic chiralities of achiral structures) or defined as direction-independent properties by averaging the responses among all structure orientations. Though of great significance for various applications, chirality extremization (maximized or minimized) with respect to incident directions or structure orientations has not been explored, especially in a systematic manner. In this study we examine the chiral responses of open photonic structures from perspectives of quasinormal modes and polarization singularities of their far-field radiations. The nontrivial topology of the momentum sphere secures the existence of generic singularity directions along which mode radiations are either circularly or linearly polarized. When plane waves are incident along those directions, the reciprocity ensures ideal maximization and minimization of optical chiralities, for corresponding mode radiations of circular and linear polarizations, respectively. For directions of general elliptical polarizations, we have unveiled the subtle equality of a Stokes parameter and the circular dichroism, showing that an intrinsically (geometrically) chiral structure can unexpectedly exhibit no optical chirality at all or even optical chiralities of opposite handedness for different incident directions. The framework we establish can be applied to not only finite scattering bodies but also infinite structures, encompassing both intrinsic and extrinsic optical chiralities. We have effectively merged two vibrant disciplines of chiral and singular optics, which can potentially trigger more optical chirality-singularity related interdisciplinary studies.

DOI: 10.1103/PhysRevLett.126.253901

Optical responses of photonic structures are generally anisotropic, depending on both polarizations and incident directions of the exciting waves. Chiralities emerge when optical responses are distinct for circularly polarized waves of opposite handedness while having the same incident direction [1,2]. Chiral effects can be observed for both intrinsically chiral and achiral structures [3–8]. For chiral structures, (intrinsic) chiralities are generally present and can be quantified as direction-independent properties through orientation-averaging chiral effects [1,2,9–12]; while for achiral structures, (extrinsic) chiralities only emerge for symmetry-breaking incident directions [13–17], which nevertheless would be absent for symmetry-preserving directions or when orientation averaged. For both scenarios, chiral responses are generally dependent on structure orientations, and thus it is fundamental to ask, given an optical structure, how its chiral response can be ideally extremized with respect to incident directions?

Besides chiral optics, another photonic branch of singular optics has also gained enormous momentum from two decades of explosive developments of nanophotonics, fertilizing many related disciplines [18–21]. Vectorial optical singularities correspond to states of circular and linear polarizations, for which semimajor axes and orientation planes of polarization ellipses are undefined, respectively [22–24]. Polarization singularities are skeletons of general electromagnetic waves, which are robust against perturbations and generically manifest in both natural and artificial fields [18–21]. Despite the ubiquity of polarization singularities, it is rather unfortunate and surprising that for decades both disciplines of chiral and singular optics developed almost independently with rare crucial interactions, especially when fundamental entities of circular polarizations are shared by both fields.

Here we investigate chirality extremization, for both achiral and chiral structures, with plane waves of varying incident directions. Chiral effects are examined from perspectives of quasinormal modes (QNMs) and radiation polarization singularities. The nontrivial topology of momentum sphere has secured existences of singularity directions, as protected by the Poincaré-Hopf theorem [25–28]. For a structure supporting a dominant QNM with waves incident along singularity directions of circular and linear mode radiations, chiral effects are ideally

maximized and minimized, respectively. For directions of general elliptical polarizations, the equality of a Stokes parameter and circular dichroism is discovered, demonstrating that an intrinsically chiral structure can unexpectedly manifest no chirality or even chiralities of opposite handedness for different orientations. The chirality extremization is generically protected by reciprocity and thus broadly applicable to both extrinsic and intrinsic chiral responses.

Without loss of generality, we study reciprocal nonmagnetic structures of relative permittivity $\epsilon(\mathbf{r},\omega)$ in vacuum background of refractive index $n=1$. An open structure supports a set of QNMs characterized by eigenfield $\tilde{\mathbf{E}}_j(\mathbf{r})$ and complex eigenfrequency $\tilde{\omega}_j$ [29]. The incident plane wave is $\mathbf{E}_{\rm inc}(\mathbf{r})$, with wave vector $\mathbf{k}_{\rm inc}$, real frequency ω, and wavelength λ. Excited fields can be expanded into QNMs as $\mathbf{E}=\sum\alpha_j(\omega)\tilde{\mathbf{E}}_j(\mathbf{r})$, with excitation coefficients [29]:

$$\alpha_j(\omega)\propto\iiint_{\mathbf{V}}-i\omega[\varepsilon(\mathbf{r},\omega)-1]\mathbf{E}_{\rm inc}(\mathbf{r})\cdot\tilde{\mathbf{E}}_j(\mathbf{r})d^3\mathbf{r}, \tag{1}$$

where $\mathbf{V}$ denotes regions the structure occupies. When only one nondegenerate QNM is dominantly excited, as is the case throughout this study, the mode subscript j can be dropped. It is well known that far-field radiations of QNMs and thus the corresponding scattered fields are divergent. Several approaches exist that can overcome this difficulty [29], and a direct technique is to treat $\tilde{\mathbf{J}}(\mathbf{r})=-i\omega[\varepsilon(\mathbf{r},\omega)-1]\tilde{\mathbf{E}}(\mathbf{r})$ as source currents according to the volume equivalence theorem (Chap. 7 of Ref. [30]). They can then be expanded into electromagnetic multipoles (spherical harmonics) at real ω, based on which convergent radiated (or scattered) far fields $\tilde{\mathbf{E}}_{\rm rad}(\mathbf{r})$ can be directly calculated [31,32].

This current-radiation perspective can simplify Eq. (1) as

$$\alpha(\omega)\propto\iiint_{\mathbf{V}}\mathbf{E}_{\rm inc}(\mathbf{r})\cdot\tilde{\mathbf{J}}(\mathbf{r})d^3\mathbf{r}. \tag{2}$$

Let us assume that $\mathbf{E}_{\rm inc}$ comes from a point-dipole moment $\mathcal{P}$ ($\mathcal{P}$ locates on the transverse plane $\mathcal{P}\cdot\mathbf{k}_{\rm inc}=0$ and is in phase with $\mathbf{E}_{\rm inc}$: $\mathcal{P}\propto\mathbf{E}_{\rm inc}$) in the far zone. According to Lorentz reciprocity [33,34]:

$$\iiint_{\mathbf{V}}\mathbf{E}_{\rm inc}(\mathbf{r})\cdot\tilde{\mathbf{J}}(\mathbf{r})d^3\mathbf{r}=\tilde{\mathbf{E}}_{\rm rad}\cdot\dot{\mathcal{P}}=-i\omega\tilde{\mathbf{E}}_{\rm rad}\cdot\mathcal{P}, \tag{3}$$

where time-derivative $\dot{\mathcal{P}}$ denotes the dipolar current and $\mathbf{E}_{\rm rad}$ is the radiated field along $\mathbf{k}_{\rm rad}=-\mathbf{k}_{\rm inc}$. Since $\mathbf{E}_{\rm inc}\propto\mathcal{P}$, Eq. (3) can be converted to $\iiint_{\mathbf{V}}\mathbf{E}_{\rm inc}(\mathbf{r})\cdot\tilde{\mathbf{J}}(\mathbf{r})d^3\mathbf{r}=-i\omega\tilde{\mathbf{E}}_{\rm rad}\cdot\mathcal{P}\propto\tilde{\mathbf{E}}_{\rm rad}\cdot\mathbf{E}_{\rm inc}$, which simplifies Eq. (2) to

$$\alpha(\omega)\propto\tilde{\mathbf{E}}_{\rm rad}\cdot\mathbf{E}_{\rm inc},\qquad\mathbf{k}_{\rm inc}=-\mathbf{k}_{\rm rad}. \tag{4}$$

It means that QNM excitation efficiency for incident plane waves can be calculated directly, through the dot product of radiated and incident fields. Alternative derivations for Eq. (4), without referring to source currents of either radiated or incident fields, are presented in the Supplemental Material [35].

The validity of Eq. (4) can be checked against the simplest example of a metal bar supporting solely an electric dipole. Electric fields radiated are shown in Fig. 1(a): the dipole is vertically oriented and the fields are parallel to the lines of longitude [28,38]. Along the dipole, there are no radiations $\tilde{\mathbf{E}}_{\rm rad}=0$ and thus $\alpha=0$ according to Eq. (4). It means plane waves incident parallel to the bar will not excite it, which agrees with our conventional method of projecting the incident electric field onto the bar axis. Similar analysis can be conducted along other directions, where one linear polarization (parallel to the radiated field) excites the dipole while the other orthogonal polarization does not. The superiority of Eq. (4) to Eq. (1) is not obvious for this example but would become apparent for more sophisticated bodies.

Radiations can be always expanded into right- and left-handed circularly polarized (RCP and LCP, denoted respectively by $\circlearrowright$ and $\circlearrowleft$) components along $\mathbf{k}_{\rm rad}$: $\tilde{\mathbf{E}}_{\rm rad}=\mu\tilde{\mathbf{E}}^{\circlearrowright}_{\rm rad}+\nu\tilde{\mathbf{E}}^{\circlearrowleft}_{\rm rad}$. Here μ and ν are generally complex

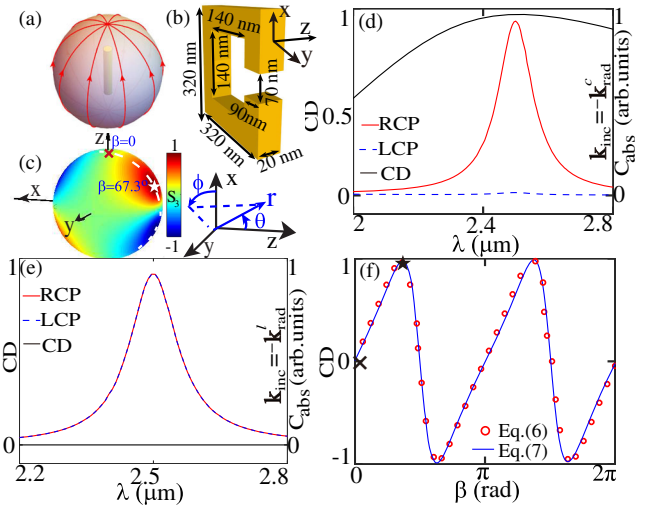

FIG. 1. (a) A metal bar supports an electric dipole mode and its radiated electric fields on the momentum sphere. (b) A gold SRR with the spherical coordinate system (r, θ, ϕ), and (c) S_3 distribution for the QNM supported. Two singularity directions are marked: $\mathbf{k}^c_{\rm rad}(\theta=67.3°,\phi=175.1°)$ ($\star$) and $\mathbf{k}^l_{\rm rad}(\theta=0)$ ($\times$). (d) and (e) CD and absorption spectra for RCP and LCP incident waves, for $\mathbf{k}_{\rm inc}=-\mathbf{k}^c_{\rm rad},-\mathbf{k}^l_{\rm rad}$, respectively [directions also marked in (f)]. (f) Angular CD spectra for waves incident antiparallel to directions on a great momentum circle marked in (c) by a dashed arc.

numbers ($|\mu^2| + |\nu^2| = 1$), the ratio between which decides properties of the polarization ellipse of $\tilde{\mathbf{E}}_{\mathrm{rad}}$ [36]. For incident RCP and LCP waves along $\mathbf{k}_{\mathrm{inc}} = -\mathbf{k}_{\mathrm{rad}}$, according to Eq. (4) excitation coefficients are, respectively,

$$\alpha^{\circlearrowleft} \propto \mu, \qquad \alpha^{\circlearrowright} \propto \nu. \tag{5}$$

When only one QNM is dominantly excited, all cross sections of extinction, scattering, and absorption are proportional to excitation efficiency $|\alpha|^2$ [35]: $\mathrm{C}^{\circlearrowleft,\circlearrowright}_{\mathrm{ext,sca,abs}} \propto |\alpha^{\circlearrowleft,\circlearrowright}|^2$. The circular dichroism (CD) is defined (similar to the Kuhn's dissymmetry factor [1]) as

$$\mathrm{CD} = (\mathrm{C}^{\circlearrowleft}_{\mathrm{abs}} - \mathrm{C}^{\circlearrowright}_{\mathrm{abs}})/(\mathrm{C}^{\circlearrowleft}_{\mathrm{abs}} + \mathrm{C}^{\circlearrowright}_{\mathrm{abs}}), \tag{6}$$

which can then be simplified through Eq. (5) as

$$\mathrm{CD} = |\mu^2| - |\nu^2| = S_3, \qquad \mathbf{k}_{\mathrm{rad}} = -\mathbf{k}_{\mathrm{inc}}. \tag{7}$$

Here, S_3 is nothing but exactly one of the Stokes parameters widely employed for polarization characterizations [36]: $S_3 = \pm 1$ corresponds, respectively, to RCP and LCP waves; $S_3 = 0$ corresponds to linear polarizations and other values of S_3 to elliptical polarizations (the difference from previous studies is that here S_3 is angular dependent). Equation (7) reveals the subtle connection between S_3 of radiations and CD when only one QNM is dominantly excited: $|\mathrm{CD}|$ can be maximized and minimized antiparallel to the **C**-direction ($S_3 = \pm 1$) and **L**-direction ($S_3 = 0$) to ideal values of $|\mathrm{CD}| = 1$ and $\mathrm{CD} = 0$, respectively. We emphasize that those chirality extremization directions are exactly where generic polarization singularities are present [22–24]. The nontrivial topology of the momentum sphere secures the existence of those singularity directions [25–28], which guarantees broad applicability of our model.

We can generalize definitions of CD to $\mathrm{CD}_{\mathrm{ext,sca}} = (\mathrm{C}^{\circlearrowleft}_{\mathrm{ext,sca}} - \mathrm{C}^{\circlearrowright}_{\mathrm{ext,sca}})/(\mathrm{C}^{\circlearrowleft}_{\mathrm{ext,sca}} + \mathrm{C}^{\circlearrowright}_{\mathrm{ext,sca}})$, and identical to Eq. (7) we have $\mathrm{CD}_{\mathrm{ext,sca}} = S_3$ [35]. Based on this relation we can deduce polarization properties of mode radiations from general scattering properties of the scatterer. For example, it has been proved that for oppositely incident waves on a reciprocal scatterer [39,40]: $\mathrm{CD}_{\mathrm{ext}}(\mathbf{k}_{\mathrm{inc}}) = \mathrm{CD}_{\mathrm{ext}}(-\mathbf{k}_{\mathrm{inc}})$, which immediately implies $S_3(\mathbf{k}_{\mathrm{rad}}) = S_3(-\mathbf{k}_{\mathrm{rad}})$ and thus Eq. (7) is actually valid for both directions of $\mathbf{k}_{\mathrm{inc}} = \pm\mathbf{k}_{\mathrm{rad}}$. It is further proved [40] that for inversion-symmetric scatterers, $\mathrm{CD}_{\mathrm{ext}} = 0$ for arbitrary incident directions, which requires that QNM is everywhere linearly polarized ($S_3 = 0$) throughout the momentum sphere [35]. It is clear from Eq. (7) that CD (including its generalized versions of $\mathrm{CD}_{\mathrm{ext,sca}}$) is solely decided by polarizations while it has nothing to do with intensities of radiations. As a result, an alternative approach for expansions of the source currents $\tilde{\mathbf{J}}(\mathbf{r})$ into multipoles of complex frequencies does not affect our results [41].

To confirm our theory, we begin with the widely employed split ring resonator (SRR) that exhibits two symmetry mirrors (**x**-**y** and **y**-**z** planes) and is thus achiral [Fig. 1(b)]. The SRR is made of gold with permittivity listed in Ref. [42]. Neighboring $\omega_1 = 7.4875 \times 10^{14}$ rad/s ($\lambda_1 = 2.516\ \mu$m), an individual QNM is excited with eigenfrequency $\tilde{\omega}_1 = (7.4875 \times 10^{14} - 2.0414 \times 10^{13} i)$ rad/s (numerical results are obtained using COMSOL Multiphysics in this study). The S_3 distribution for this mode is presented in Fig. 1(c), where polarization singularities with $S_3 = \pm 1$ or 0 are generically manifest along various directions [18–21]. Two singularity directions are marked (one **C**-direction of $\mathbf{k}^{c}_{\mathrm{rad}}$ and one **L**-direction of $\mathbf{k}^{l}_{\mathrm{rad}} \| \mathbf{z}$) and circularly polarized plane waves are incident antiparallel to those directions. The corresponding spectra of absorption and CD are demonstrated, respectively, in Figs. 1(d) and 1(e), showing clearly that $|\mathrm{CD}|$ is maximized and minimized, respectively. The deviation of CD from its ideal absolute values of 1 and 0 at some spectral positions is induced by some marginal contributions of other QNMs excited, as is also the case in following studies of other structures. We emphasize that zero CD in Fig. 1(e) is observed along $\mathbf{k}^{l}_{\mathrm{rad}}$ that preserves the mirror symmetry of the whole scattering configuration (parity conservation requires zero CD [1,40]). This is consistent with the conception that extrinsic chiralities are present along symmetry-breaking directions [14–17].

To verify the validity of Eq. (7) for general nonsingularity directions $0 < |S_3| < 1$, a great circle on the momentum sphere (parametrized by $0 \le \beta \le 2\pi$) that contains the marked **C**-direction and **L**-direction is selected [also marked in Fig. 1(c)]. The angular CD spectra ($\omega = \omega_1$) along directions antiparallel to points on this circle are shown in Fig. 1(f), where two sets of results are presented: one calculated from S_3 [Eq. (7)] and the other through $\mathrm{C}_{\mathrm{abs}}$ obtained in direct scattering simulations [Eq. (6)]. Both sets of results agree well, the symmetry of which [$\mathrm{CD}(\beta) \approx \mathrm{CD}(\beta \pm \pi)$] reconfirms our previous claims of $\mathrm{CD}(\mathbf{k}_{\mathrm{inc}}) = \mathrm{CD}(-\mathbf{k}_{\mathrm{inc}})$ and $S_3(\mathbf{k}_{\mathrm{rad}}) = S_3(-\mathbf{k}_{\mathrm{rad}})$ for single mode excitations.

Now that achiral structures do exhibit chiral responses along some incident directions, why should they be classified as achiral? The conventional standard is purely geometric: they exhibit mirror or inversion symmetries and thus can be superimposed onto their mirror images [1]. Alternatively, CD can be employed to categorize structures as chiral or not, but only when it is orientation averaged among all incident directions:

$$\mathbb{CD} = \frac{1}{4\pi |\mathbf{k}_{\mathrm{inc}}|^2} \iint \mathrm{CD}\, d^2\mathbf{k}_{\mathrm{inc}}. \tag{8}$$

The law of parity conservation [1,40] ensures that the mirror-symmetry or inversion-symmetry operation maps $\mathrm{C}^{\circlearrowleft,\circlearrowright}_{\mathrm{abs}}$ to $\mathrm{C}^{\circlearrowright,\circlearrowleft}_{\mathrm{abs}}$, flipping the sign of CD according to Eq. (6).

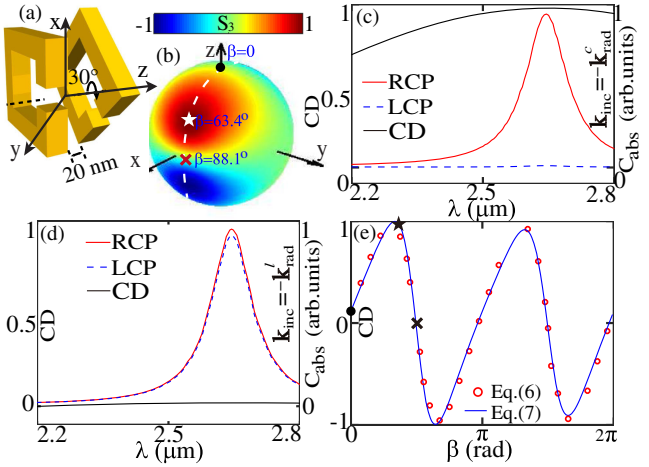

FIG. 2. (a) An intrinsically chiral SRR dimer and (b) S_3 distribution for the QNM supported. Two singularity directions are marked: $\mathbf{k}^{c}_{rad}(\theta = 63.4°, \phi = 7.3°)$ ($\star$) and $\mathbf{k}^{l}_{rad}(\theta = 88.1°, \phi = 7.3°)$ ($\times$). (c) and (d) CD and absorption spectra for circularly polarized incident waves, for $\mathbf{k}_{inc} = -\mathbf{k}^{c}_{rad}, -\mathbf{k}^{l}_{rad}$, respectively [directions also marked in (e)]. (e) Angular CD spectra for waves incident antiparallel to directions on a great momentum circle marked in (b) by a dashed arc.

As a result, $\mathbb{CD} = 0$ for mirror-symmetric or inversion-symmetric structures, which agrees with the geometric standard of image superimposition.

Now we turn to a SRR dimer that is intrinsically chiral [Fig. 2(a)], which supports a QNM at eigenfrequency $\tilde{\omega}_2 = (7.0765 \times 10^{14} - 1.6125 \times 10^{13}\mathrm{i})$ rad/s. The S_3 distribution of this QNM is presented in Fig. 2(b), where one **C**-direction and one **L**-direction are marked. The corresponding spectra of absorption and CD are demonstrated respectively, in Figs. 2(c) and 2(d) for plane waves incident antiparallel to those directions. We have also selected a great momentum circle [as marked in Fig. 2(b), containing **C**-direction, **L**-direction and the **z**-axis] and the corresponding angular CD spectra [$\omega = \mathrm{Re}(\tilde{\omega}_2)$ and $\lambda = 2.662$ μm, where Re denotes the real part] along directions antiparallel to points on this circle are shown in Fig. 2(e). It is worth noting that along the dimer twisting direction (**z** axis with $\beta = 0$ and π), CD is actually quite small ($\mathrm{CD} = S_3 = 0.12$) and far from being maximal.

For chiral structures consisting of twisted elements that are similar to that shown in Fig. 2(a), though not stated explicitly, it is widely believed that the incident direction of maximal |CD| should be parallel to the twisting axis [2–4,6,7,43–49]. In fact, this is not the case and CD along other directions can be much more significant as shown in Fig. 2(e). A structure being achiral or chiral can be defined optically through whether or not $\mathbb{CD} = 0$, and the sign of $\mathbb{CD}$ rather than that of CD is connected to such a defined handedness. Meanwhile, we have to emphasize that even the sign of $\mathbb{CD}$ can be opposite at different spectral potions due to dispersions [1], telling that there is basically no definitive correspondence between geometric handedness and the chiral responses. For achiral structures, $\mathbb{CD} = 0$ does not require $\mathrm{CD} = 0$ everywhere, and extrinsic chiralities emerge along directions of $\mathrm{CD} \neq 0$ [13–17]. In a similar fashion, for chiral structures, $\mathbb{CD} \neq 0$ requires neither $\mathrm{CD} \neq 0$ nor $\mathbb{CD}$ and CD being of the same sign everywhere. This means that an intrinsically chiral structure can manifest no chirality at all ($\mathrm{CD} = 0$) or even chiralities of opposite handedness (CD of different signs) among different incident directions [Fig. 2(e)].

Up to now, we have discussed how to extremize CD to its ideal absolute maximum or minimum values with respect to incident directions. Since $|\mathbb{CD}|$ is automatically minimized ($\mathbb{CD} = 0$) for achiral structures, it is both interesting and significant to ask how to maximize $|\mathbb{CD}|$ ideally to $\mathbb{CD} = \pm 1$. According to Eq. (8), the ideal maximization of $|\mathbb{CD}|$ requires $\mathrm{CD} = \pm 1$ along all incident directions [or more accurately some isolated directions can be exempted, as they do not affect the overall integration in Eq. (8)]. This requires that mode radiations are circularly polarized with the same handedness throughout the momentum sphere except for some isolated directions. This is possible, for example, for a pair of parallel electric and magnetic dipoles (or higher-order multipoles of the same order) of the same magnitude (in terms of total radiated power) and $\pm\pi/2$ phase contrast, as secured by the electromagnetic duality symmetry (along the isolated directions parallel to the dipole orientation direction there are no radiations and thus the polarizations are not defined) [38]. Our conclusions for $|\mathbb{CD}|$ maximization are consistent with the results presented in Ref. [50], where the problem has been approached from a very different perspective. However, up to now, most if not all realistic reciprocal structures are anisotropic in terms of CD responses and thus ideal $\mathbb{CD} = \pm 1$ has not been obtained so far, though it is not theoretically impossible.

As a final step, we proceed to apply our framework to infinitely extended photonic crystal slabs (PCSs), which support Bloch QNMs [21,51,52]. It is well known that through symmetry breaking, some bound states in the continuum [52] can be broken into circularly polarized radiating states [21,27,53–57]. One such square-latticed (periodicity $p = 380$ nm) PCS of index $n = 2.02$ is inset in Fig. 3(a), which is achiral (symmetric with respect to the **x**-**y** and **y**-**z** planes) while the symmetry respect to the **x**-**z** plane is broken. The dispersion curve [$\mathrm{Re}(\tilde{\omega})$ versus $\mathbf{k}^{x}_{rad}$, with $\mathbf{k}^{y}_{rad} = 0$] that is colored according to the S_3 distribution of QNM radiations for one nondegenerate TE-like (electric fields distributed on the **x**-**y** plane) band are shown in Fig. 3(a). One **C** direction is marked ($\star$) with $\tilde{\omega}_3 = (3.8409 \times 10^{15} - 1.8686 \times 10^{13}\mathrm{i})$ rad/s and $\mathbf{k}^{c}_{rad} = (\mathbf{k}^{c,x}_{rad}, \mathbf{k}^{c,y}_{rad}, \mathbf{k}^{c,z}_{rad})$, with $\mathbf{k}^{c,x}_{rad} p/2\pi = 0.1332$, $\mathbf{k}^{c,y}_{rad} = 0$, $\mathbf{k}^{c,z}_{rad} = \sqrt{[\mathrm{Re}(\tilde{\omega}_3)/c]^2 - (\mathbf{k}^{c,x}_{rad})^2 - (\mathbf{k}^{c,y}_{rad})^2}$ and c is the speed of light. Now we shine circularly polarized plane waves onto the PCS with fixed frequency $\omega = \mathrm{Re}(\tilde{\omega}_3)$ along different directions (variant $\mathbf{k}^{x}_{inc}$) on the **x**-**z** plane

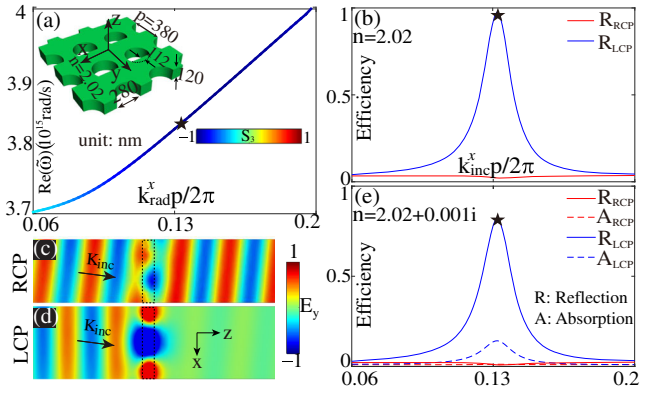

FIG. 3. (a) The dispersion curve of one TE-like QNM band for square-latticed PCS (show schematically as inset). The S_3 distribution of the QNM band is also shown and a singularity direction $\mathbf{k}^c_{\mathrm{rad}}$ is marked ($\star$). (b) Angular reflection spectra for RCP and LCP incident waves without material losses, and (c)–(d) corresponding near-field distributions when $\mathbf{k}_{\mathrm{inc}} = \mathbf{k}^c_{\mathrm{rad}}$. (e) Angular absorption and reflection spectra with material losses.

($\mathbf{k}^y_{\mathrm{inc}} = 0$), with $\mathbf{k}_{\mathrm{inc}} = (\mathbf{k}^x_{\mathrm{inc}}, \mathbf{k}^y_{\mathrm{inc}}, \mathbf{k}^z_{\mathrm{inc}})$. Angular reflection ($R$) spectra are presented in Fig. 3(b), where the critical direction $\mathbf{k}_{\mathrm{inc}} = \mathbf{k}^c_{\mathrm{rad}}$ is marked.

Figure 3(b) shows clearly that along **C** direction RCP and LCP waves are almost fully transmitted and reflected (no higher-order diffractions), respectively. Near-field distributions ($\mathbf{E}_y$ on the **x**-**z** plane; dashed rectangles denote the cross sections of the PCS) are presented in Figs. 3(c) and 3(d), where the formation of a standing wave upon reflection in Fig. 3(d) obscures the information of oblique incidence. Those properties agree with our result in Eq. (4), which requires that circularly polarized Bloch QNM is maximally and not excited by LCP and RCP waves, leading to perfect reflection and transmission, respectively. When material losses are incorporated ($n = 2.02 + 0.001i$), both spectra of reflection (R) and absorption (A) efficiency are summarized in Fig. 3(e). Along the marked critical direction, as expected, there is considerable and almost no absorption for incident LCP and RCP waves, respectively, which is also consistent with our previous analyses.

To conclude, we revisit optical chiralities from perspectives of polarization singularities. When waves are incident parallel to the **C** and **L** directions, the chiral responses are ideally extremized. For general incident directions, we discover the subtle equivalence of CD and S_3, showing that an intrinsically chiral structure can surprisingly manifest no chirality at all or even chiralities of opposite handedness among different directions. The validity of our conclusions resides on the approximation of single QNM excitation, which is indeed applicable to many structures, especially to those that do not exhibit any geometric symmetries (*e.g.*, rotational symmetries that protect at least one pair of degenerate QNMs [49]). When several QNMs (including degenerate ones) are co-excited, observable optical properties are neither proportional to the excitation efficiency of any QNM nor their direct sum, since QNMs are generally not orthogonal and inter-mode interference terms have to be carefully examined [29,31,58]. Besides QNM-based approaches [29,31,59], techniques such as the scattering matrix method [60] can be also employed to tackle more general scenarios, from which to extract simple and general principles constitutes a promising research direction. Our results are directly applicable to elliptical dichroism [35], and singularity based approaches we introduce can be potentially extended to structured non-plane beams [61,62].

We acknowledge the financial support from National Natural Science Foundation of China (Grants No. 11874026 and No. 11874426), and several other Researcher Schemes of the National University of Defense Technology. W. L. is indebted to Sir Michael Berry and Professor Tristan Needham for invaluable correspondence.

*These authors contributed equally to this work.
†yuntian@hust.edu.cn
‡wei.liu.pku@gmail.com

[1] L. D. Barron, *Molecular Light Scattering and Optical Activity* (Cambridge University Press, Cambridge, England, 2009).
[2] *Singular and Chiral Nanoplasmonics*, edited by S. Boriskina and N. I. Zheludev, 1st ed. (Jenny Stanford Publishing, Singapore, 2014).
[3] M. Hentschel, M. Schäferling, X. Duan, H. Giessen, and N. Liu, Chiral plasmonics, Sci. Adv. **3**, e1602735 (2017).
[4] J. T. Collins, C. Kuppe, D. C. Hooper, C. Sibilia, M. Centini, and V. K. Valev, Chirality and chiroptical effects in metal nanostructures: Fundamentals and current trends, Adv. Opt. Mater. **5**, 1700182 (2017).
[5] Y. Luo, C. Chi, M. Jiang, R. Li, S. Zu, Y. Li, and Z. Fang, Plasmonic chiral nanostructures: Chiroptical effects and applications, Adv. Opt. Mater. **5**, 1700040 (2017).
[6] M. Qiu, L. Zhang, Z. Tang, W. Jin, C.-W. Qiu, and D. Yuan Lei, 3D metaphotonic nanostructures with intrinsic chirality, Adv. Funct. Mater. **28**, 1803147 (2018).
[7] J. Mun, M. Kim, Y. Yang, T. Badloe, J. Ni, Y. Chen, C.-W. Qiu, and J. Rho, Electromagnetic chirality: From fundamentals to nontraditional chiroptical phenomena, Light Sci. Appl. **9**, 139 (2020).
[8] L. V. Poulikakos, P. Gutsche, K. M. McPeak, S. Burger, J. Niegemann, C. Hafner, and D. J. Norris, Optical chirality flux as a useful far-field probe of chiral near fields, ACS Photonics **3**, 1619 (2016).
[9] I. Fernandez-Corbaton, M. Fruhnert, and C. Rockstuhl, Dual and chiral objects for optical activity in general scattering directions, ACS Photonics **2**, 376 (2015).
[10] E. Vinegrad, D. Vestler, A. Ben-Moshe, A. R. Barnea, G. Markovich, and O. Cheshnovsky, Circular dichroism of single particles, ACS Photonics **5**, 2151 (2018).

[11] R. N. S. Suryadharma, C. Rockstuhl, O. J. F. Martin, and I. Fernandez-Corbaton, Quantifying Fano properties in self-assembled metamaterials, Phys. Rev. B **99**, 195416 (2019).
[12] A. Fazel-Najafabadi, S. Schuster, and B. Auguié, Orientation averaging of optical chirality near nanoparticles and aggregates, arXiv:2012.10010.
[13] A. Papakostas, A. Potts, D. M. Bagnall, S. L. Prosvirnin, H. J. Coles, and N. I. Zheludev, Optical Manifestations of Planar Chirality, Phys. Rev. Lett. **90**, 107404 (2003).
[14] E. Plum, V. A. Fedotov, and N. I. Zheludev, Optical activity in extrinsically chiral metamaterial, Appl. Phys. Lett. **93**, 191911 (2008).
[15] E. Plum, X.-X. Liu, V. A. Fedotov, Y. Chen, D. P. Tsai, and N. I. Zheludev, Metamaterials: Optical Activity Without Chirality, Phys. Rev. Lett. **102**, 113902 (2009).
[16] I. Sersic, M. A. van de Haar, F. B. Arango, and A. F. Koenderink, Ubiquity of Optical Activity in Planar Metamaterial Scatterers, Phys. Rev. Lett. **108**, 223903 (2012).
[17] C. Rizza, A. Di Falco, M. Scalora, and A. Ciattoni, One-Dimensional Chirality: Strong Optical Activity in Epsilon-Near-Zero Metamaterials, Phys. Rev. Lett. **115**, 057401 (2015).
[18] G. J. Gbur, *Singular Optics* (CRC Press Inc., Boca Raton, 2016).
[19] M. Berry, *Half-Century of Physical Asymptotics and Other Diversions: Selected Works by Michael Berry* (World Scientific Publishing Company, Singapore, 2017).
[20] M. R. Dennis, K. O'Holleran, and M. J. Padgett, Chapter 5 Singular optics: Optical vortices and polarization singularities, in *Progress in Optics*, Vol. 53, edited by E. Wolf (Elsevier, Amsterdam, 2009), pp. 293–363.
[21] W. Liu, W. Liu, L. Shi, and Y. Kivshar, Topological polarization singularities in metaphotonics, Nanophotonics, **10** 1469 (2021).
[22] J. F. Nye, Polarization effects in the diffraction of electromagnetic waves: The role of disclinations, Proc. R. Soc. A **387**, 105 (1983).
[23] J. F. Nye, Lines of circular polarization in electromagnetic wave fields, Proc. R. Soc. A **389**, 279 (1983).
[24] M. V. Berry, Geometry of phase and polarization singularities illustrated by edge diffraction and the tides, in *Second International Conference on Singular Optics (Optical Vortices): Fundamentals and Applications*, Vol. 4403 (International Society for Optics and Photonics, Cardiff, 2001), pp. 1–12.
[25] W. Chen, Y. Chen, and W. Liu, Singularities and Poincaré Indices of Electromagnetic Multipoles, Phys. Rev. Lett. **122**, 153907 (2019).
[26] T. Needham, *Visual Differential Geometry and Forms: A Mathematical Drama in Five Acts* (Princeton University Press, Princeton, 2021).
[27] W. Chen, Y. Chen, and W. Liu, Line singularities and Hopf indices of electromagnetic multipoles, Laser Photonics Rev. **14**, 2000049 (2020).
[28] W. Chen, Q. Yang, Y. Chen, and W. Liu, Global Mie scattering: Polarization morphologies and the underlying topological invariant, ACS Omega **5**, 14157 (2020).
[29] P. Lalanne, W. Yan, K. Vynck, C. Sauvan, and J.-P. Hugonin, Light interaction with photonic and plasmonic resonances, Laser Photonics Rev. **12**, 1700113 (2018).
[30] C. A. Balanis, *Advanced Engineering Electromagnetics*, 2nd ed. (Wiley, Hoboken, N.J, 2012).
[31] D. A. Powell, Interference Between the Modes of an All-Dielectric Meta-Atom, Phys. Rev. Applied **7**, 034006 (2017).
[32] P. Grahn, A. Shevchenko, and M. Kaivola, Electromagnetic multipole theory for optical nanomaterials, New J. Phys. **14**, 093033 (2012).
[33] L. D. Landau, L. P. Pitaevskii, and E. M. Lifshitz, *Electrodynamics of Continuous Media: Volume 8*, 2nd ed. (Butterworth-Heinemann, Amsterdam, 1984).
[34] R. J. Potton, Reciprocity in optics, Rep. Prog. Phys. **67**, 717 (2004).
[35] See Supplemental Material at http://link.aps.org/supplemental/10.1103/PhysRevLett.126.253901 that includes the following four sections: (I) Alternative derivations for Eq. (4) without involving source currents; (II) Verifications of $\mathrm{CD}_{\mathrm{ext,sca}} = S_3$ for both achiral and chiral scatterers; (III) S_3 distributions of an inversion-symmetric scatterer and its CD responses; (IV) Applications for elliptical dichroism maximization. Supplemental Material includes Refs. [32,36,37].
[36] A. Yariv and P. Yeh, *Photonics: Optical Electronics in Modern Communications*, 6th ed. (Oxford University Press, New York, 2006).
[37] A. T. de Hoop, A reciprocity theorem for the electromagnetic field scattered by an obstacle, Appl. Sci. Res. **8**, 135 (1960).
[38] J. D. Jackson, *Classical Electrodynamics*, 3rd ed. (Wiley, New York, 1998).
[39] D. L. Sounas and A. Alù, Extinction symmetry for reciprocal objects and its implications on cloaking and scattering manipulation, Opt. Lett. **39**, 4053 (2014).
[40] W. Chen, Q. Yang, Y. Chen, and W. Liu, Scattering activities bounded by reciprocity and parity conservation, Phys. Rev. Research **2**, 013277 (2020).
[41] T. Wu, A. Baron, P. Lalanne, and K. Vynck, Intrinsic multipolar contents of nanoresonators for tailored scattering, Phys. Rev. A **101**, 011803(R) (2020).
[42] P. B. Johnson and R. W. Christy, Optical constants of the noble metals, Phys. Rev. B **6**, 4370 (1972).
[43] J. K. Gansel, M. Thiel, M. S. Rill, M. Decker, K. Bade, V. Saile, G. von Freymann, S. Linden, and Martin Wegener, Gold helix photonic metamaterial as broadband circular polarizer, Science **325**, 1513 (2009).
[44] M. Schäferling, D. Dregely, M. Hentschel, and H. Giessen, Tailoring Enhanced Optical Chirality: Design Principles for Chiral Plasmonic Nanostructures, Phys. Rev. X **2**, 031010 (2012).
[45] X. Yin, M. Schäferling, B. Metzger, and H. Giessen, Interpreting chiral nanophotonic spectra: The plasmonic Born-Kuhn model, Nano Lett. **13**, 6238 (2013).
[46] Y. Cui, L. Kang, S. Lan, S. Rodrigues, and W. Cai, Giant chiral optical response from a twisted-arc metamaterial, Nano Lett. **14**, 1021 (2014).

[47] Z. Wang, H. Jia, K. Yao, W. Cai, H. Chen, and Y. Liu, Circular dichroism metamirrors with near-perfect extinction, ACS Photonics **3**, 2096 (2016).

[48] A. F. Najafabadi and T. Pakizeh, Analytical chiroptics of 2D and 3D nanoantennas, ACS Photonics **4**, 1447 (2017).

[49] M. V. Gorkunov, A. A. Antonov, and Y. S. Kivshar, Metasurfaces with Maximum Chirality Empowered by Bound States in the Continuum, Phys. Rev. Lett. **125**, 093903 (2020).

[50] I. Fernandez-Corbaton, M. Fruhnert, and C. Rockstuhl, Objects of Maximum Electromagnetic Chirality, Phys. Rev. X **6**, 031013 (2016).

[51] J. Joannopoulos, S. Johnson, J. Winn, and R. Meade, *Photonic Crystals: Molding the Flow of Light—Second Edition*, 2nd ed. (Princeton University Press, Princeton, 2008).

[52] C. W. Hsu, B. Zhen, A. Douglas Stone, J. D. Joannopoulos, and M. Soljačić, Bound states in the continuum, Nat. Rev. Mater. **1**, 16048 (2016).

[53] W. Liu, B. Wang, Y. Zhang, J. Wang, M. Zhao, F. Guan, X. Liu, L. Shi, and J. Zi, Circularly Polarized States Spawning from Bound States in the Continuum, Phys. Rev. Lett. **123**, 116104 (2019).

[54] C. Guo, M. Xiao, Y. Guo, L. Yuan, and S. Fan, Meron Spin Textures in Momentum Space, Phys. Rev. Lett. **124**, 106103 (2020).

[55] X. Yin, J. Jin, M. Soljačić, C. Peng, and B. Zhen, Observation of topologically enabled unidirectional guided resonances, Nature (London) **580**, 467 (2020).

[56] W. Ye, Y. Gao, and J. Liu, Singular Points of Polarizations in the Momentum Space of Photonic Crystal Slabs, Phys. Rev. Lett. **124**, 153904 (2020).

[57] T. Yoda and M. Notomi, Generation and Annihilation of Topologically Protected Bound States in the Continuum and Circularly Polarized States by Symmetry Breaking, Phys. Rev. Lett. **125**, 053902 (2020).

[58] P. T. Leung, S. Y. Liu, and K. Young, Completeness and orthogonality of quasinormal modes in leaky optical cavities, Phys. Rev. A **49**, 3057 (1994).

[59] F. Alpeggiani, N. Parappurath, E. Verhagen, and L. Kuipers, Quasinormal-Mode Expansion of the Scattering Matrix, Phys. Rev. X **7**, 021035 (2017).

[60] M. I. Mishchenko, L. D. Travis, and A. A. Lacis, *Scattering, Absorption, and Emission of Light by Small Particles*, 1st ed. (Cambridge University Press, Cambridge, New York, 2002).

[61] X. Zambrana-Puyalto, X. Vidal, and G. Molina-Terriza, Angular momentum-induced circular dichroism in non-chiral nanostructures, Nat. Commun. **5**, 4922 (2014).

[62] J. Ni, S. Liu, D. Wu, Z. Lao, Z. Wang, K. Huang, S. Ji, J. Li, Z. Huang, Q. Xiong, Y. Hu, J. Chu, and C.-W. Qiu, Gigantic vortical differential scattering as a monochromatic probe for multiscale chiral structures, Proc. Natl. Acad. Sci. U.S.A. **118**, e2020055118 (2021).